PHOTOPOLYMERS BASED ON ETHYNYL-FUNCTIONALIZED DEGRADABLE POLYLACTIDES BY THIOL-YNE 'CLICK CHEMISTRY'

Alberto Concellón,[a] Laura Asín,[b, c] Sandra González-Lana,[d] Jesús M. de la Fuente,[b, c] Carlos Sánchez-Somolinos,[d,*] Milagros Piñol[a] and Luis Oriol[a,*]

[a] Departamento de Química Orgánica, Instituto de Ciencia de Materiales de Aragón (ICMA)-Facultad de Ciencias, Universidad de Zaragoza-CSIC, 50009, Pedro Cerbuna 12, Zaragoza, Spain.

[b] Instituto de Ciencia de Materiales de Aragón (ICMA), Universidad de Zaragoza-CSIC, 50009, Zaragoza, Spain.

[c] CIBER in Bioengineering, Biomaterials and Nanomedicine (CIBER-BBN).

[d] Instituto de Ciencia de Materiales de Aragón (ICMA), Universidad de Zaragoza-CSIC, Departamento de Física de la Materia Condensada, Facultad de Ciencias, Pedro Cerbuna 12, 50009, Zaragoza, Spain.

* Corresponding author. Email: loriol@unizar.es, carloss@unizar.es

ABSTRACT

This work reports the synthesis and characterization of a series of new biodegradable ethynyl-ended polylactides with different architectures. These ethynyl-functionalized polylactides were blended with a commercial low molar mass tetrathiol to prepare crosslinked polymeric networks by thiol-yne photoclick reaction that was studied by infrared spectroscopy and photocalorimetry. Cell proliferation assays with human colorectal carcinoma cells showed that the resulting polymeric networks are not cytotoxic. Two-dimensional structures were prepared by patterned curing using direct laser writing of the photopolymerizable formulations. Preliminary cell tests on substrates provided with these polymeric structures demonstrate the possibility to generate cell patterns.

GRAPHICAL ABSTRACT

Photopolymers based on ethynyl-functionalized degradable polylactides by thiol-yne 'click chemistry'

Alberto Concellón, Laura Asín, Sandra González-Lana, Jesús M. de la Fuente, Carlos Sánchez-Somolinos, Milagros Piñol, and Luis Oriol**

We have demonstrated the preparation of new crosslinked polymeric networks using ethynyl-functionalized polylactides and a commercial low molar mass tetrathiol by thiol-yne photoclick reaction. We have prepared two-dimensional structures using direct laser writing. The resulting materials are not cytotoxic and can be of interest for cell patterning.

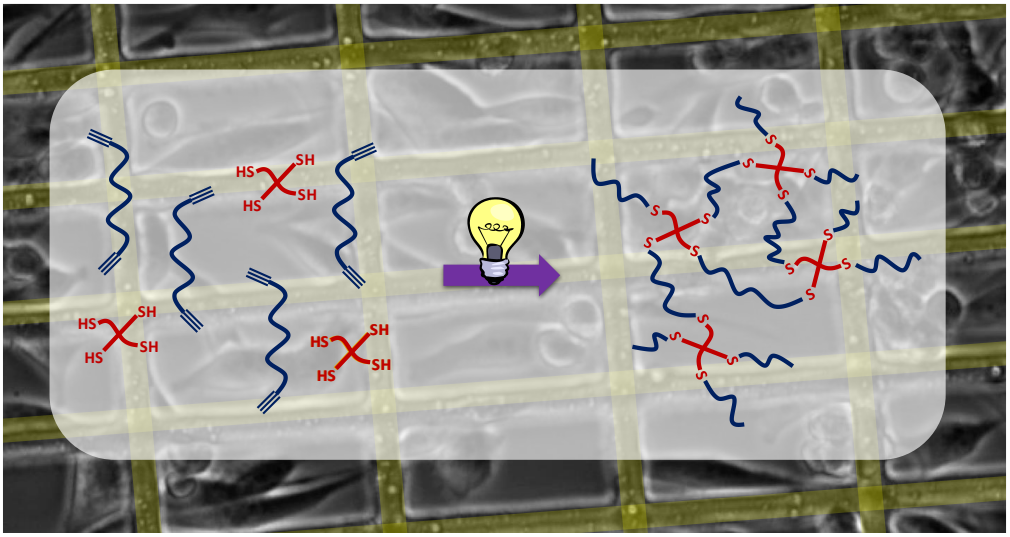

KEYWORDS

Thiol-yne Click Chemistry; Microstructuring; Polylactides

1. Introduction

In recent years, there has been an emerging interest in the development of biomaterials based on the use of biodegradable polymers for applications such as tissue engineering or drug delivery, among others.[1-4] Crosslinked polymeric materials are particularly attractive in this field since the chemical structure and architecture of polymers can be easily controlled and their final properties tailored to fulfill the performance requirements of target applications. Together, crosslinks impart mechanical and temporal stability to the final system. From the different strategies, light-induced crosslinking is particularly attractive as it can be temporally and spatially controlled on exposing the material to the initiating light source.[5-7]

For the preparation of crosslinked biomaterials, photopolymerization of multifunctional (meth)acrylate monomers has been mostly used.[8-15] However, despite the demonstrated advantages of the *in situ* formed (meth)acrylate-based networks, the reaction that proceeds through a radical chain-growth polymerization mechanisms generates non-biodegradable high molecular mass acrylic chains.[16, 17] These acrylic chains become the major drawback as they are difficult to eliminate from the body.

As an alternative, Anseth and Bowman developed degradable networks formed by a photoinitiated thiol-ene reaction.[18-22] Using a low molecular mass multifunctional thiol with hydrolyzable ester groups and an alkene-functionalized biodegradable macromonomer, a highly crosslinked network was obtained. Degradation of such network resulted in low molecular weight byproducts that are easier to excrete from the body. Additionally, the robust nature of thiol-ene chemistry allows the preparation of well-defined materials for applications in a wide range of disciplines.[23, 24]

Similarly, the analogous thiol-yne photoreaction can also lead to highly crosslinked polymer networks.[25-29] Nonetheless, in a light induced thiol-yne polymerization, two thiols react with one ethynyl group giving polymer networks with higher crosslinking densities than the equivalent thiol-ene networks.[27] Additionally, the versatility of this chemistry facilitates post-polymerization modification of residual functional groups to produce materials with improved and tailored properties, as it has be recently pointed by Quick *et al* on the preparation and subsequent dual-postfuncionalization of micro-resolved 3D mesostructures prepared by thiol-yne chemistry using low molecular weight monomers as photoresist systems.[30] The radical mechanism of the thiol-yne reaction makes it a very reliable and versatile method that tolerates a variety of functional groups, which is of interest for the synthesis of new functional materials.[31-34] Very recently Blasco *et al* reviewed the formation of precision polymeric networks using advanced photoinduced ligation techniques including thiol-yne approach, as emerging and promising alternatives to acrylate or epoxy materials.[7] Regardless the benefits, the preparation of degradable polymer networks by thiol-yne photocrosslinking of biodegradable polymers has not been so frequently exploited.[35, 36] In a previous work,[37] we first demonstrated that the thiol-yne photoreaction was an attractive tool for the preparation of biocompatible crosslinked polymeric materials for cell patterns. The investigated system comprised an ethynyl-functionalized hyperbranched aliphatic polyester and a non-cytotoxic, commercial and multifunctional low molecular mass thiol (as crosslinker of the hyperbranched polyester). Recently, Oesterreicher *et al* explored this chemistry for the 3D printing of tailor-made medical devices using low molecular weight monomers and studied the mechanical properties of the obtained networks and their biodegradability.[38, 39] Even the thiol-yne chemistry was successfully applied to the

covalent post-functionalization of polylactide surfaces to yield antibacterial surfaces.[40]

In this work, we report the preparation of polymeric networks by thiol-yne photoclick reaction of ethynyl-functionalized polylactides (PLAs) and a low molar mass tetrathiol. Thus, the synthesis of a series of amorphous biodegradable ethynyl-ended polylactides (PLAs) has been approached by ring opening polymerization (ROP) of *D,L*-lactide and post-polymerization modification of the macromolecule ends. By using different hydroxy-functionalized initiators, PLAs with different architectures have been prepared that include several linear PLAs differing in the number of terminal ethynyl groups (**L$_X$-YNE** and **LB$_X$-YNE** with two and four ethynyl groups, respectively), and four arm star PLAs also having four terminal ethynyl groups (**ST$_X$-YNE**) (**Scheme 1**). These PLAs were combined with a commercial low molar mass tetrathiol, which has been previously used in the preparation of biomaterials,[18, 20, 37, 38] to prepare polymeric networks. The photopolymerization process was investigated by infrared spectroscopy (FTIR) and photocalorimetry (photo-DSC). Thermal properties of PLA precursors and resulting photocrosslinked networks were characterized by DSC. To assess their biocompatibility, cell viability experiments were performed on photocrosslinked thin films of these materials. In addition, the possibility to prepare two-dimensional patterned surfaces of these materials using direct laser writing (DLW) and cell culture on them was also explored.

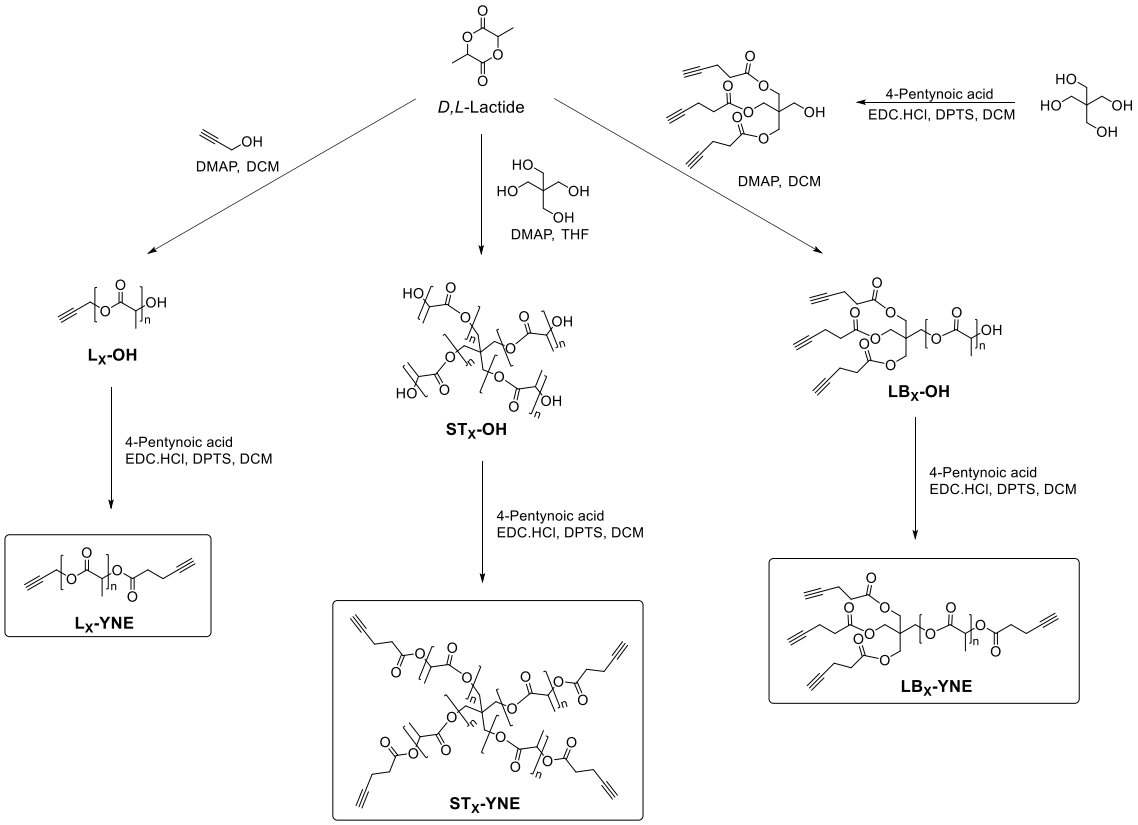

Scheme 1. Chemical structure and synthesis of ethynyl-functionalized PLAs

2. Experimental

2.1. Materials

D,L-Lactide (Sigma-Aldrich) was dried under vacuum at 30ºC for 24 hours before use. All other commercially available starting materials were purchased from Sigma-Aldrich and used as received. Pentaerythritol tetrakis(3-mercaptopropionate), which was also purchased from Sigma-Aldrich, was used as a crosslinker and Irgacure 369 (Ciba) was used as photoinitiator.

2.2. Synthesis of pentaerythritol tris(4-pentynoate)

4-(Dimethylamino)pyridinium *p*-toluenesulfonate (DPTS) (6.37 g, 20.39 mmol), pentaerythritol (1.85 g, 13.59 mmol), and 4-pentynoic acid (5.00 g, 50.97 mmol) were dissolved in dry THF (100 mL). The reaction flask was cooled in an ice bath and flushed with argon, then *N*-(3-dimethylaminopropyl)-*N′*-ethylcarbodiimide

hydrochloride (9.77 g, 50.97 mmol) was added. The mixture was stirred at r.t. for 24 h under argon atmosphere. Then, the solvent was evaporated under reduced pressure. The crude product was dissolved in DCM and washed twice with water and once with brine. Finally, the organic layer was dried over anhydrous magnesium sulfate and the solvent was evaporated. The crude product was purified by flash column chromatography on silica gel using hexane/ethyl acetate (2:1) as eluent. Yield: 14%. IR (KBr, ν, cm^{-1}): 3503, 3292, 1735, 1188, 1089. ^{1}H NMR ($CDCl_3$, 400 MHz, δ, ppm): 4.19 (s, 6H), 3.56 (d, 2H, J=6.9 Hz), 2.62-2.48 (m, 12H), 2.39 (t, 1H, J=6.9 Hz), 2.00 (t, 3H, J=2.6 Hz).^{13}C NMR ($CDCl_3$, 100 MHz, δ, ppm): 171.8, 82.3, 69.6, 62.5, 60.8, 44.1, 33.4, 14.6. Anal. calcd for $C_{20}H_{24}O_7$: C, 63.82%; H, 6.43%. Found: C, 64.21%; H, 6.31%.

2.3. General polymerization procedure

A solution of the alcohol and 4-(dimethylamino)pyridine ($[alcohol]_0$:$[DMAP]_0$ = 0.5) in dry DCM was dried under argon atmosphere over 4Å molecular sieves during 12 h. Lactide and this solution were added to a Schlenk flask that was then closed with a rubber septum. The flask was deoxygenated by three freeze-pump-thaw cycles and flushed with argon. The reaction was stirred at 35 ºC until disappearance of the lactide signals in ^{1}H NMR spectrum. Then, the reaction mixture was washed twice with 1N hydrochloric acid and once with brine. Finally, the organic layer was dried over anhydrous magnesium sulfate and the solvent was partially evaporated. The polymer was precipitated by adding the solution dropwise to cold methanol and further centrifugation at 4000 rpm for 30 min. The polymer was washed twice with cold methanol and dried under vacuum at room temperature. Yield: 32-74%

2.4. General procedure for the esterification of hydroxy-functionalized polylactides with 4-pentynoic acid

4-(Dimethylamino)pyridinium *p*-toluenesulfonate (DPTS) (0.025 M), the hydroxy-functionalized PLA (0.05 M) and 4-pentynoic acid (0.1 M) were dissolved in dry DCM. The reaction flask was cooled in an ice bath and flushed with argon, then *N*-(3-dimethylaminopropyl)-*N′*-ethylcarbodiimide hydrochloride (0.1 M) was added. The reaction mixture was stirred at r.t. until the disappearance of the methine signal corresponding to the terminal lactide unit in ^{1}H NMR spectrum. Then, the reaction was washed twice water and once with brine. Finally, the organic layer was dried over anhydrous magnesium sulfate and the solvent was partially evaporated. The polymer was precipitated by adding the solution dropwise to cold methanol and further centrifugation at 4000 rpm for 30 min. The polymer was washed twice with cold methanol and dried under vacuum at room temperature. Yield: 42-80%

2.5. Characterization Techniques

FTIR spectra were obtained on a Bruker Vertex 70 FT-IR spectrophotometer using KBr pellets or polymer films deposited onto KBr pellets by casting, in the 4000-400 cm^{-1} region, with 4 cm^{-1} accuracy. Solution NMR experiments were carried out on Bruker Avance spectrometers operating at 400 MHz for ^{1}H and 100 for ^{13}C, using standard pulse sequences. Chemical shifts are given in ppm relative to TMS and the solvent residual peak was used as internal reference. Elemental analysis was performed using a Perkin-Elmer 2400 microanalyzer. MALDI-TOF MS was performed on an Autoflex mass spectrometer (Bruker Daltonics) using dithranol as matrix. Molar masses and dispersities were determined using Polytools 1.15 (Bruker Daltonics). Size exclusion chromatography (SEC) was carried out on a Waters e2695 Alliance liquid chromatography system equipped with a Waters 2424 evaporation light scattering detector using two Styragel columns, HR4 and HR1 from Waters. Measurements were performed in THF with a flow of 1 mL min^{-1} using PMMA narrow molecular weight

standards. Thermogravimetric analysis (TGA) were performed using a Q5000IR from TA instruments at heating rate of 10 ºC min^{-1} under a nitrogen atmosphere. Thermal transitions were determined by differential scanning calorimetry (DSC) using a DSC Q2000 from TA instruments with powdered samples (2−5 mg) sealed in aluminum pans. Glass transition temperatures (T_g) were determined at the half height of the baseline jump. Photo-DSC experiments were carried out by casting the photocrosslinkable solution onto an aluminum capsule. The light source was a photocalorimetry accessory from TA Instruments composed by a 200 W high pressure Hg source provided with a 250-450 nm filter. Light was transmitted to the sample through an extended range, dual-quartz light guide. Samples for hydrolytic degradation were prepared by casting-deposition of the photopolymerizable formulation onto glass substrates. Polymeric films were crosslinked at 100 ºC with 10 minutes of UV irradiation. Hydrolytic degradation of each sample was performed immersing the polymeric network in phosphate buffered solution (pH 7.4, containing 0.02% NaN_3) at 37 ºC. After hydrolytic degradation, the samples were rinsed with fresh distilled water and soaked in fresh distilled water twice for 1 h, and then dried under reduced pressure for at least 3 days.

2.6. Cell culture

Human colorectal carcinoma cells transfected with Green Fluorescent Protein (GFP) (HCT 116-GFP) were cultured in Dulbecco's modified Eagle's medium (DMEM, Lonza, BE12-614F) supplemented with 10% fetal bovine serum (FBS), 1% Glutamine and 1% of a mixture of penicillin and streptomycin. Cells were maintained under 37 °C and 5% CO_2 conditions.

2.7. Cell viability

Formulations of the ethynyl-functionalized **ST$_2$-YNE** PLA with a stoichiometric amount of the commercial thiol crosslinker (stoichometry alkyne/thiol 1:2) and 3 wt. % of photoinitiator were used for these studies. Thin photopolymerizable films for cell viability assays were prepared by casting the photopolymer formulation onto a glass cover-slip using dichloromethane as solvent. The glass slides were previously silanized with (3-mercaptopropyl)trimethoxysilane.[41] After solvent evaporation at RT, films were flood exposed with light coming from an EXFO Onmicure S-2000 lamp equipped with a UV bandpass filter (320-390 nm). The power on the sample was 10 mW/cm^2 applied for 600s.

Cell viability after different incubation times on thin films of photocrosslinked PLA based material was analysed by Trypan Blue exclusion method. Photocrosslinked PLA films were sterilized in a laminar flow cabinet under UV light 20 minutes each side and placed in sterilized plates. Three 24-well plates were prepared; 10^5, $6{\cdot}10^4$, $4{\cdot}10^4$ cells per well were seeded for the three incubation times (24, 48 and 72 h) respectively. Total final volume was 500 μL per well. Control samples contained cells attached to glass coverslips in the same conditions as the rest of samples were also prepared.

After the selected incubation times, medium supernatant, washing supernatants and cells split up with trypsin were collected in the same tube, centrifuged and resuspended in 200 μL of growth medium. Cell suspensions were mixture with Trypan Blue (1:1) and counted in a Neubaüer chamber. Each sample was prepared in triplicate. The relative cell viability was calculated as: live cells / total cells x 100.

2.8. Direct laser writing (DLW)

Microstructuring was conducted using a DLW home-built setup based on a 355nm wavelength CW laser (Zouk CW 355 nm DPSSL from Cobolt, Stolna, Sweden). The

laser delivers a 10mW, 0.7 mm diameter beam. The laser energy is adjusted by using a UV neutral density filter wheel. The attenuated laser beam is focused using a UV focusing x10 microscope objective (Thorlabs LMU-10X-NUV). The position of the objective lens is adjusted along the Z-direction using a Z-axis translation mount. Sample positioning is done using a computer controlled XY translation stage (ANT130-110-XY-PLUS from Aerotech, Pittsburgh, PA, USA).

The laser power and the scan speed during the laser writing process was adjusted for each of the mixtures. As an example, for the formulation comprising the macromonomer **ST$_2$-YNE** with a stoichiometric amount of the thiolated crosslinker (2 thiol groups for each alkyne) with 3 wt % of Irgacure 369 photoinitiator, the power at the entrance of the objective was 0.6 mW with a laser scanning speed of 15 mm/s. After the direct laser writing process is completed and in order to develop the structure, the unreacted material was removed by dipping and gently moving the film in acetone for 20 s. followed by a gently flush with isopropyl alcohol. Immediately after the development step, drying of the films was carried out by exposing them to an air flow for approximately one minute. To ensure elimination of solvent residues, the films were stored overnight in a vacuum oven at RT.

2.9. Surface topography characterization

Topographic characterization of the 2D microstructures obtained through DLW was performed using a Dual Sensofar PLμ2300 microscope working in confocal mode.

2.10. Adhesion study

HCT 116-GFP cells were split up from culture flasks with trypsin and counted in a Neubaüer chamber. $5 \cdot 10^4$ cells were placed in each well of a 24 well plate that contained the coverslips were the PLA resins with the microstructures were prepared.

The total volume of each well was 500 μL. After an incubation of time of 48 h cells were washed twice with PBS in order to remove not adherent ones and then cells were fixed with 4% paraformaldehyde (PFA) 15 min at room temperature. After fixation cells were washed three times with PBS and observed by optical microscopy.

3. Results and Discussion

3. 1. Synthesis and characterization of ethynyl-functionalized polylactides

D,L-Lactide was polymerized by organocatalyzed ROP using propargyl alcohol as initiator (**Scheme 1**) to produce α-ethynyl-ω-hydroxy-functionalized linear PLAs **Lx-OH**. The polymerizations were conducted in dry dichloromethane (DCM) using 4-(dimethylamino)pyridine (DMAP) in a 2:1 molar ratio relative to the initiating alcohol.[42] PLAs with average molar masses, M_n, of approx. 1000, 2000 and 4000 g mol^{-1} were obtained by appropriately varying the [monomer]:[initiator] ratio (**Table 1**). Polymerization progress was followed by ^{1}H NMR by monitoring the consumption of the lactide monomer. After 48 hours, *D,L*-lactide signals were not detected indicating a complete conversion.

Table 1. Number average molar masses (M_n) and thermal properties of the obtained PLAs

Polymer	[Lactide]:[initiator][a]	M_n^{theo} [b]	M_n^{NMR} [c]	M_n^{SEC} [d]	$Đ$[d]	T_g (°C)[e]
L_1-OH	7	1100	1500	3000	1.17	28
L_2-OH	14	2100	2400	4200	1.15	32
L_3-OH	28	4100	4200	7800	1.12	38
L_1-YNE	-	-	1600	3600	1.13	31
L_2-YNE	-	-	2400	4900	1.11	37
L_3-YNE	-	-	4200	9400	1.11	42
LB_1-OH	14	2400	2500	4600	1.07	30
LB_2-OH	28	4400	4300	6600	1.10	31
LB_1-YNE	-	-	2700	4900	1.08	36

LB$_2$-YNE	-	-	4500	7100	1.10	37
ST$_1$-OH	28	4200	4100	5900	1.07	29
ST$_2$-OH	56	8200	7400	13500	1.08	39
ST$_1$-YNE	-	-	4500	5900	1.07	31
ST$_2$-YNE	-	-	7800	14200	1.09	40

[a] Monomer to initiator (R-OH) molar ratio feed at the polymerization

[b] Theoretical molar mass (conversion = 1) calculated according to formula $M_n^{theo} = \frac{[monomer]}{[initiator]} \times conversion \times M_{monomer} + M_{initiator}$

[c] M_n^{NMR} determined by ^{1}H NMR spectroscopy: $M_n^{NMR} = n \times \frac{M_{monomer}}{2} + M_{initiator}$

[d] M_n^{SEC} and $Đ$ were calculated by SEC using THF (1 mL min^{-1}) as the mobile phase relative to PMMA standards.

[e] Glass transition temperature determined at the half height of the baseline jump on the second heating scan at 10ºC min^{-1}

^{1}H NMR spectra of **Lx-OH** polymers show the signals attributable to the PLA backbone along with minor signals corresponding to the end groups coming from the initiator (**Figures S1-S2** in Supporting Information). As a representative example, the ^{1}H NMR spectrum of **L$_1$-OH** is shown in **Figure 1a**. The average number molar masses, M_n, of the PLAs were determined by end group analysis with ^{1}H NMR spectroscopy (M_n^{NMR} in **Table 1**) using the relative integration of the signals corresponding to polymer backbone and end groups. The polymerizations were well controlled as demonstrated by the close agreement between experimental molar masses (M_n^{NMR}) and the theoretical ones calculated on the basis of a monomer conversion of 1 (M_n^{theo} in **Table 1**).

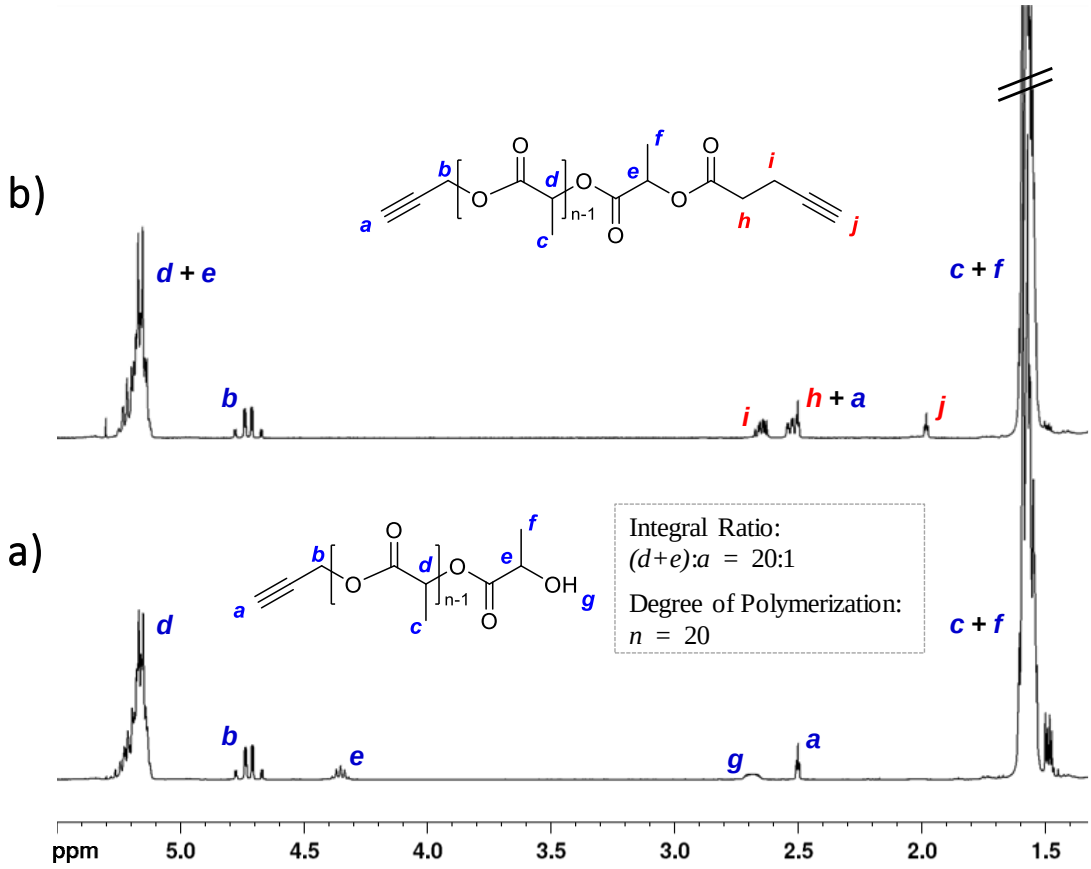

Figure 1. a) ^{1}H NMR spectrum (400 MHz, $CDCl_3$) recorded for **L_1-OH** (the degree of polymerization (n) was calculated from the relative integration of signals *d, e* and *a*). **b)** ^{1}H NMR spectrum (400 MHz, $CDCl_3$) recorded for **L_1-YNE** (the degree of esterification was calculated from the relative integration of signals *b* and *j*).

Esterification of the terminal hydroxyl group of the **L_X-OH** PLAs with 4-pentynoic acid was carried out using *N*-(3-dimethylaminopropyl)-*N*′-ethylcarbodiimide hydrochloride (EDC·HCl) as acid activating agent and 4-(dimethylamino)-pyridinium 4-toluenesulfonate (DPTS) as catalyst (**Scheme 1**). The progress of the reaction was monitored by ^{1}H NMR, following the disappearance of −CH− proton (*e* in **Figure 1a**) of the terminal lactide unit. Newly appearing signals at 1.98 (protons *j* in **Figure 1b**) and 2.46-2.69 ppm (protons *i* and *h*) corresponding to the incorporated 4-pentynoate terminal ester were employed to evaluate the degree of terminal alkynyl groups incorporated by post-functionalization (**Figures S3-S4** in Supporting Information). The

relative integration of the signals, confirms a quantitative esterification of hydroxyl groups with 4-pentynoic acid.

To increase the number of ethynyl terminal groups, pentaerytritol tris(4-pentynoate) was used as initiator to produce **LB$_X$-OH** PLAs with M_n of around 2000 and 4000 g mol^{-1} (**Scheme 1**) using the polymerization conditions established for the corresponding **L$_X$-OH**. However, in this case longer reaction times (up to 6 days) were needed to achieve complete conversion (see **Figure S5**), probably because the initiating alcohol is more sterically hindered. **LB$_X$-YNE** PLAs, with four terminal ethynyl groups, were subsequently synthesized by quantitative esterification of the terminal hydroxyl groups of the **LB$_X$-OH** with 4-pentynoic acid using EDC·HCl and DPTS.

Alternatively, PLAs with four ethynyl end groups were also obtained by using pentaerythritol as initiator in the ROP of *D,L*-Lactide, and subsequent esterification of the terminal hydroxyl groups with 4-pentynoic acid (**Scheme 1**). Two PLAs (**ST$_X$-OH**) of around 1000 or 2000 g mol^{-1} in each arm (similar to **L$_1$-OH** and **L$_2$-OH**) were prepared using the same reaction conditions as for the corresponding **L$_X$-OH**. After that, the four ethynyl terminal groups were incorporated by post-functionalization obtaining **ST$_X$-YNE** PLAs.

The average molar masses of PLAs were also estimated by MALDI-TOF mass spectroscopy and the values were in accordance with the NMR values (**Figures S14-S27** in Supporting Information). The SEC curves showed monomodal molar mass distributions with low polydispersity values ($Đ$ < 1.15), as expected for a controlled polymerization (**Figure S28**). The relative number molar masses estimated by SEC using PMMA standards (M_n^{SEC}) are gathered in **Table 1**.

The thermal analysis of all synthesized PLAs was undertaken by thermogravimetric analysis (TGA) and differential scanning calorimetry (DSC) (**Table**

1). Weight losses associated to the presence of residual solvents or water were not detected and all materials showed good thermal stability up to around 200ºC. All these polymers were amorphous materials as deduced from the DSC curves where clear baseline jumps corresponding to the glass transition (T_g) were only observed just above room temperature. As expected the molar mass of the PLAs has an influence on the T_g, and low molar mass PLAs exhibit lower T_gs than PLAs with higher molar mass but related polymeric topology. Besides, ethynyl-functionalized PLAs display slightly higher T_gs values than their hydroxyl-functionalized precursors.

3. 2. Study of the thiol-yne photocrosslinking process

Photopolymerizable formulations were prepared by blending the ethynyl-functionalized PLA with a stoichiometric amount of the crosslinker pentaerythritol tetrakis(3-mercaptopropionate) (**Figure S29a**) (given that one ethynyl group reacts with two thiol groups) and 3 wt. % of the photoinitiator (Irgacure 369, **Figure S29b**) in DCM, and subsequently evaporation of the solvent at room temperature.[37]

The photoinduced thiol-yne click reaction was studied by FTIR using films of the photopolymerizable formulations prepared by casting-deposition onto KBr pellets. Before UV irradiation, IR spectra of the films presented the C_{sp}–H *st* vibration band (at around 3300 cm^{-1}) of the alkyne terminal groups of PLA, and the S–H *st* vibration band (at around 2600 cm^{-1}) of the thiol groups of the crosslinker. Films were initially photopolymerized at 25ºC (**Figure S30** in Supporting Information) but there was not a significant conversion after 1 min of UV irradiation. In the FTIR spectra, the intensity of the C_{sp}–H *st* and S–H *st* vibration bands diminished because of thiol addition to alkyne group but they were still observed indicating that the reaction was not completed. This fact can be ascribed to the low diffusion of the reactive groups in the bulk as the viscosity increases when the photocrosslinking reaction proceeds. In order to

reach higher conversions, films were UV irradiated at 100 ºC (above T_g) for 10 min observing how the C_{sp}–H *st* and S–H *st* vibration bands disappeared (**Figure 2a**). A control experiment was carried by annealing at 100ºC a film without UV-irradiation to discard the concurrence of thermally induced crosslinking (**Figure S31** in Supporting Information). The FTIR results concluded that at 100ºC the alkyne-thiol addition was photoinduced.

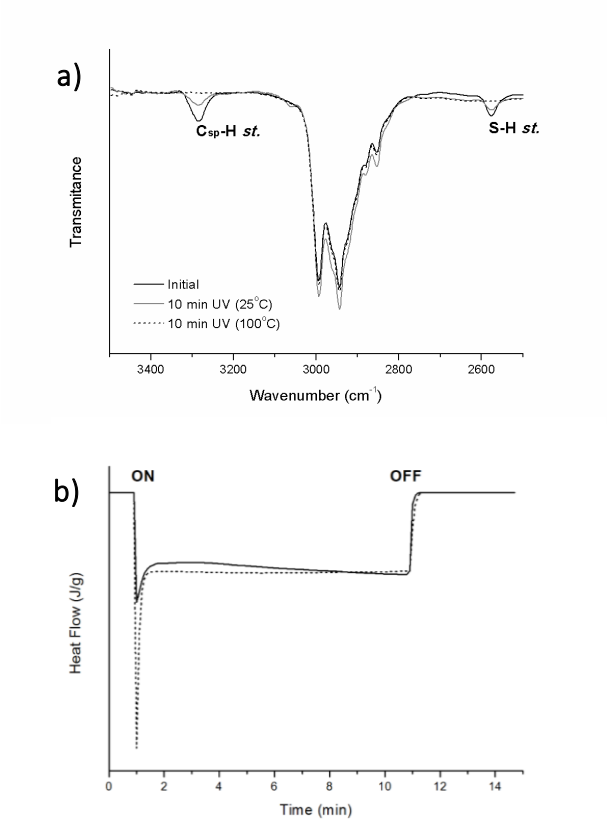

Figure 2. a) FTIR spectra of a **ST$_2$-YNE** photopolymerizable film cast on a KBr pellet before UV irradiation (black line), after UV irradiation at 25ºC for 10 min (grey line) and after UV irradiation at 100ºC for 10 min (dashed line). **b)** Photo-DSC curve registered during the photoinduced crosslink by thiol-yne addition of a **ST$_2$-YNE** photopolymerizable film at 25ºC (solid line) or 100ºC (dashed line). On/off indicates switching on and off the UV lamp (no thermal crosslinking is detected at 100ºC before switching on the lamp).

The photocrosslinking process was also monitored by photo-DSC at 25ºC and 100ºC (**Figure 2b**). The DSC curves showed an intense exotherm on exposing the

sample to the UV light due to the heat evolved on the alkyne-thiol addition. The reaction proceeds rapidly and is completed after approx. 1-2 min. As it can be deduced from the area of the peaks, higher conversions were reached at 100ºC than at 25ºC in accordance with FTIR studies.

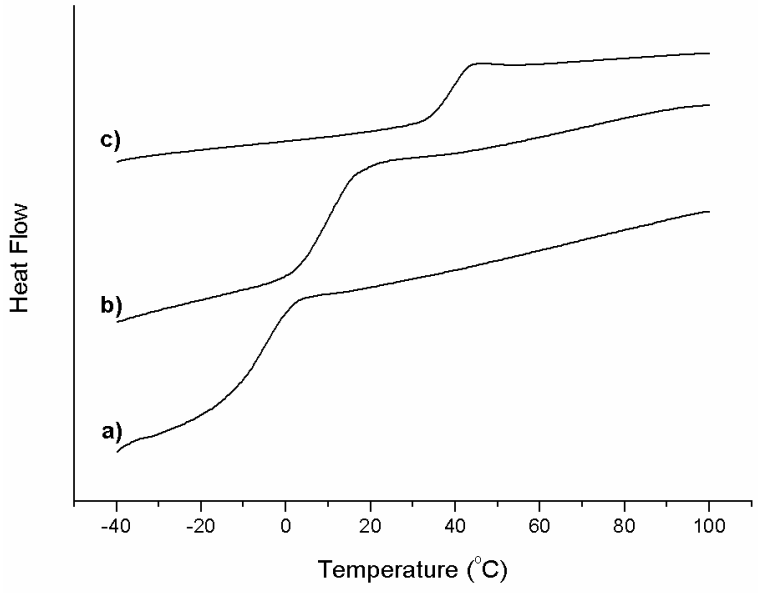

Figure 3. DSC traces of **(a) ST_2-YNE** photopolymerizable formulation**, (b) ST_2-YNE** photocrosslinked at 25ºC, **(c) ST_2-YNE** photocrosslinked at 100ºC corresponding to the first heating scan (10ºC min^{-1}).

The thermal analysis of the photopolymerizable formulations and the resulting crosslinked polymers at 25ºC and at 100ºC was carried out by DSC (**Figure 3**). The photopolymerizable formulations (i.e. before photocrosslinking) presented a T_g at around –5ºC, clearly lower than the corresponding alkyne-functionalized PLA due to the presence of the liquid tetrathiol added to the formulation. By crosslinking an increase of the T_g was perceived compared to the initial formulations observing also that films crosslinked at 100ºC showed higher values of T_g than those prepared at 25ºC, due to higher conversions reached at 100ºC. The final T_g values of the films crosslinked at 100ºC were similar to the corresponding PLA precursors.

L_1-YNE was selected to evaluate the hydrolytic degradation of the thiol-yne photocrosslinked networks. The degradation study was carried out by preparing crosslinked photopolymer films onto glass substrates that were immersed at 37ºC in a pH=7.4 phosphate buffer containing 0.02% NaN_3 to prevent bacteria growing. The weight loss [Weight loss (%) = $(W_0–W_t)/W_0$, being W_0 and W_t the initial and remaining weights of the films, respectively] was monitored till complete degradation (**Figure S32**). No significant weight loss was observed during the first 10 weeks (around 4%). The onset of weight loss was detected at week 10-15. The weight loss was observed up to week 30 when completed.

3. 3. Cell viability studies

Cell viability studies were conducted on **ST_2-YNE** based crosslinked films, taking this material as a model system. Films were prepared on top of glass slides that were previously silanized with (3-mercaptopropyl)trimethoxysilane to promote covalent bonding of the crosslinked polymeric network with the glass after UV curing. The use of untreated glass slides led to photopolymerized films that easily detach after some time when exposed to water. Cell viability studies were performed using Human colorectal carcinoma cells transfected with Green Fluorescent Protein (GFP) (HCT 116-GFP). After incubating cells on thin films of **ST_2-YNE** based crosslinked material for 24, 48 and 72 h, cell viability was analysed by Trypan Blue and results are presented in **Figure 4**. Trypan Blue molecules enter into cells only when the cell membrane is disrupted resulting in blue dyed cells, on the contrary, viable cells with intact plasmatic membrane do not present any staining. The viability values of cells cultured on photocrosslinked films were similar to values that correspond to control cells, reaching almost 100% of viability. So, with these results, we can confirm that this material is not

toxic, in terms of plasmatic membrane integrity, for these cells at the selected incubation times.

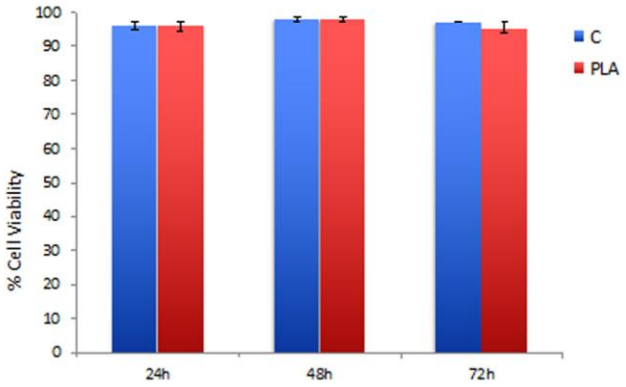

Figure 4. Cell viability analyzed by Trypan Blue exclusion method after incubating HTC 116-GFP cells on thin films of crosslinked **ST$_2$-YNE** PLA based photopolymer 24, 48 and 72 h. Each sample was made in triplicate. (C are the cell cultures on the control samples and PLA the ones on the crosslinked films of the **ST$_2$-YNE** PLA based photopolymer).

3. 4. Direct laser writing experiments

The ability of these thiol-yne systems to generate microstructures was explored using direct laser writing (DLW). Films of the photopolymerizable formulations, obtained by casting, with typical thickness in the order of 3 - 5 microns were structured using the DLW setup described in the experimental section. Briefly, a 355 nm continuous wave (CW) laser beam was focused on a photopolymerizable film by using a ×10 objective. Patterned samples were prepared by moving the thin film of the photopolymerizable material within the focal plane using a computer controlled XY translation stage. Photopolymerization selectively took place in the exposed areas remaining the non-exposed material unreacted. This unexposed material was subsequently etched away using acetone as solvent. Silanization of the glass substrates was again needed in order to ensure attachment of the microstructures after wet etching. **Figure 5** shows confocal microscope images of crossing lines obtained using this technique on two different

formulations prepared from two different macromers with low and high degree of functionality, **L_1-YNE** (**Figure 5a**) and **ST_2-YNE** (**Figure 5b**) respectively, a stoichiometric amount of the thiol and 3 wt % of photoinitiator (Irgacure 369). Well-defined structures were obtained after the washing step. Slightly thicker regions are observed in the intersection of two perpendicular lines what is ascribed to partial removal of material from the directly exposed areas during the solvent etching step.[37] Although higher doses can be applied to improve curing in the lines and minimize this partial etching effect, this usually resulted in undesired curing in the non-directly exposed areas leading to non well-defined cured microstructures. Also the cured lines showed, after wet etching, a more rounded height profile for the **L_1-YNE** when compared to **ST_2-YNE** as shown in the right side of **Figure 5**. This difference can be ascribed to the different degree of functionality of the two reactive PLA with **L_1-YNE** having two reactive ethynyl groups while **ST_2-YNE** has four alkyne groups. Higher degree of crosslinking in **ST_2-YNE** based material, compared to that derived from **L_1-YNE**, leads to a higher stability against solvent etching.

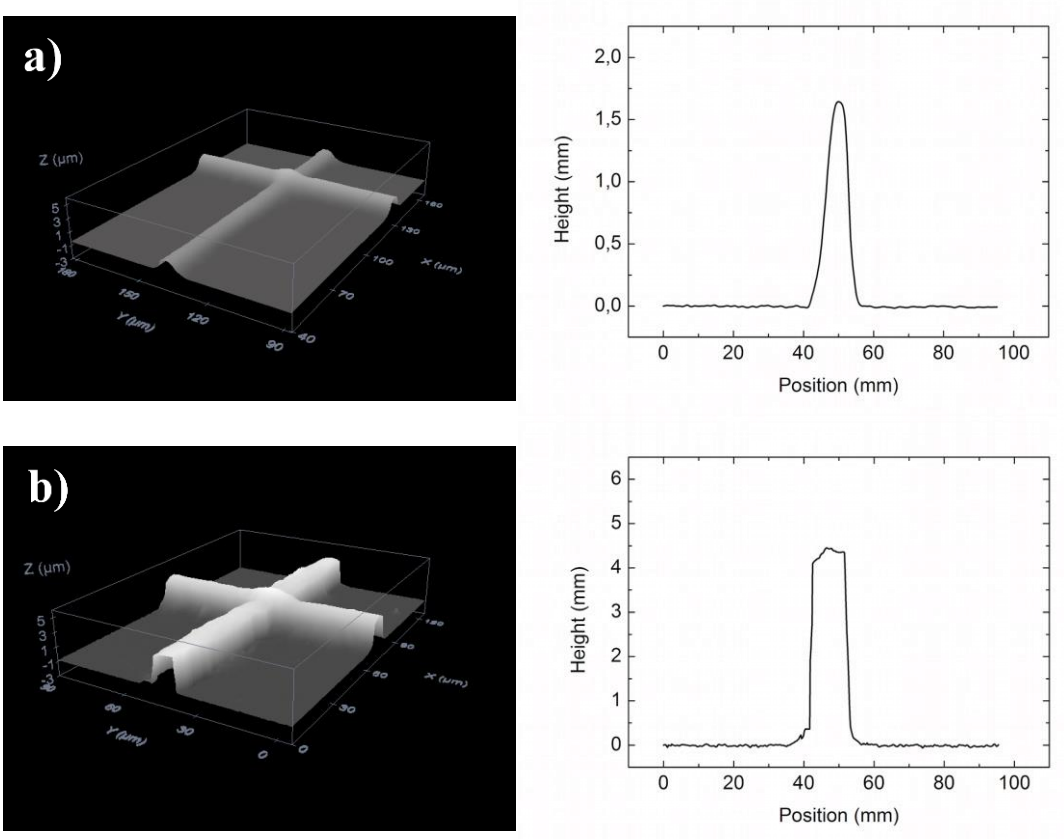

Figure 5. Topography images of crossing lines (left) and height profile of individual lines (right) generated by direct laser writing using a formulation comprising the macromonomer a) **L_1-YNE** and b) **ST_2-YNE**, both with a stoichiometric amount of the thiol (stoichometry alkyne/thiol 1:2) and 3 wt % of photoinitiator. Images were obtained using a confocal microscope.

Cell culturing was preliminarily carried out on **ST_2-YNE** PLA patterned substrates for 48 h and cell morphology was observed by optical microscopy. **Figure 6** shows how cells look to be confined into the microstructures but not attached to the edges and not grown onto the structures protrusions. It seems that cells are inside the limits of structures just because a matter of space but not because any specific affinity that make cells to follow the stripe direction. Different widths of the stripes were studied and similar effect was detected. No differences between different microstructures dimensions were observed, cells were not oriented to the stripes in any

of them but attached on the surface, well attached confined into the structures but randomly elongated.

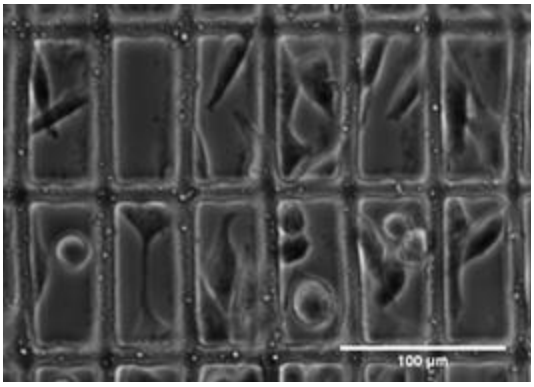

Figure 6. Cells cultured on substrates with different widths PLA microstructures after 48 h.

4. Conclusions

The synthesis and characterization of alkyne end-functionalized polylactides having different architectures was accomplished by ROP and subsequent esterification of terminal hydroxyl groups. These polylactides were used as biodegradable macromonomers in the preparation of photopolymerizable formulations using a low molecular weight tetrathiol that reacts with the alkyne end-groups of the polylactide to yield a crosslinked network. The photoclick reaction was monitored by IR spectroscopy and photo-DSC. In order to achieve a complete conversion, the reaction was carried out at 100ºC, but a thermal induced reaction was rejected, which allow using these photopolymerizable formulations for the preparation of patterned structures.

Cell viability assays performed on thin films of PLA based crosslinked material resulting have shown that the resulting materials are not cytotoxic. The presented results demonstrate that these materials combined with advanced photolithographic techniques allow the microfabrication of well-defined micrometre scale structures of interest for cell patterning.

ACKNOWLEDGEMENTS

This work was supported by the MINECO, Spain, under the project MAT2014-55205-P, SAF2014-54763-C2-2-R, FEDER funding and Aragón Government-FSE (Research Groups E04 and E93). The authors would also like to acknowledge the use of the CEQMA Services (Nuclear Magnetic Resonance, Mass Spectra, Surface and Coatings Characterization and Thermal Analysis) of the Universidad de Zaragoza-CSIC. A. Concellón thanks MINECO for his PhD grant. L. Asín acknowledges her Juan de la Cierva fellowship.

REFERENCES

[1] H.-J. Yoon, W.-D. Jang, Polymeric supramolecular systems for drug delivery, J. Mater. Chem. 20 (2010) 211-222.

[2] J.H. Park, S. Lee, J.-H. Kim, K. Park, K. Kim, I.C. Kwon, Polymeric nanomedicine for cancer therapy, Prog. Polym. Sci. 33 (2008) 113-137.

[3] M.C. Serrano, E.J. Chung, G.A. Ameer, Advances and Applications of Biodegradable Elastomers in Regenerative Medicine, Adv. Funct. Mater. 20 (2010) 192-208.

[4] D. Puppi, F. Chiellini, A.M. Piras, E. Chiellini, Polymeric materials for bone and cartilage repair, Prog. Polym. Sci. 35 (2010) 403-440.

[5] S.J. Bryant, K.S. Anseth, The effects of scaffold thickness on tissue engineered cartilage in photocrosslinked poly(ethylene oxide) hydrogels, Biomaterials 22 (2001) 619-626.

[6] J.A. Burdick, K.S. Anseth, Photoencapsulation of osteoblasts in injectable RGD-modified PEG hydrogels for bone tissue engineering, Biomaterials 23 (2002) 4315-4323.

[7] E. Blasco, M. Wegener, C. Barner-Kowollik, Photochemically Driven Polymeric Network Formation: Synthesis and Applications, Adv. Mater. (2017) DOI:10.1002/adma.201604005.

[8] J. Kopecek, Hydrogels: From soft contact lenses and implants to self-assembled nanomaterials, J. Polym. Sci. Part A: Polym. Chem. 47 (2009) 5929-5946.

[9] K.S. Masters, D.N. Shah, L.A. Leinwand, K.S. Anseth, Crosslinked hyaluronan scaffolds as a biologically active carrier for valvular interstitial cells, Biomaterials 26 (2005) 2517-2525.

[10] D.N. Shah, S.M. Recktenwall-Work, K.S. Anseth, The effect of bioactive hydrogels on the secretion of extracellular matrix molecules by valvular interstitial cells, Biomaterials 29 (2008) 2060-2072.

[11] J. Zhu, Bioactive modification of poly(ethylene glycol) hydrogels for tissue engineering, Biomaterials 31 (2010) 4639-4656.

[12] Y. Ikada, H. Tsuji, Biodegradable polyesters for medical and ecological applications, Macromol. Rapid Commun. 21 (2000) 117-132.

[13] S. Li, Hydrolytic degradation characteristics of aliphatic polyesters derived from lactic and glycolic acids, J. Biomed. Mater. Res. 48 (1999) 342-353.

[14] A.P. Gupta, V. Kumar, New emerging trends in synthetic biodegradable polymers - Polylactide: A critique, Eur. Polym. J. 43 (2007) 4053-4074.

[15] J.D. Clapper, J.M. Skeie, R.F. Mullins, C.A. Guymon, Development and characterization of photopolymerizable biodegradable materials from PEG–PLA–PEG block macromonomers, Polymer 48 (2007) 6554-6564.

[16] B. Baroli, Photopolymerization of biomaterials: issues and potentialities in drug delivery, tissue engineering, and cell encapsulation applications, J. Chem. Technol. Biotechnol. 81 (2006) 491-499.

[17] A.T. Metters, C.N. Bowman, K.S. Anseth, A Statistical Kinetic Model for the Bulk Degradation of PLA-b-PEG-b-PLA Hydrogel Networks, J. Phys. Chem. B 104 (2000) 7043-7049.

[18] A.E. Rydholm, C.N. Bowman, K.S. Anseth, Degradable thiol-acrylate photopolymers: polymerization and degradation behavior of an in situ forming biomaterial, Biomaterials 26 (2005) 4495-4506.

[19] S.K. Reddy, K.S. Anseth, C.N. Bowman, Modeling of network degradation in mixed step-chain growth polymerizations, Polymer 46 (2005) 4212-4222.

[20] A.E. Rydholm, S.K. Reddy, K.S. Anseth, C.N. Bowman, Development and characterization of degradable thiol-allyl ether photopolymers, Polymer 48 (2007) 4589-4600.

[21] A.A. Aimetti, A.J. Machen, K.S. Anseth, Poly(ethylene glycol) hydrogels formed by thiol-ene photopolymerization for enzyme-responsive protein delivery, Biomaterials 30 (2009) 6048-6054.

[22] T.Y. Lee, J. Carioscia, Z. Smith, C.N. Bowman, Thiol−Allyl Ether−Methacrylate Ternary Systems. Evolution Mechanism of Polymerization-Induced Shrinkage Stress and Mechanical Properties, Macromolecules 40 (2007) 1473-1479.

[23] C.E. Hoyle, C.N. Bowman, Thiol-Ene Click Chemistry, Angew. Chem. Int. Ed. 49 (2010) 1540-1573.
[24] M.J. Kade, D.J. Burke, C.J. Hawker, The power of thiol-ene chemistry, J. Polym. Sci. Part A: Polym. Chem. 48 (2010) 743-750.
[25] J.W. Chan, H. Zhou, C.E. Hoyle, A.B. Lowe, Photopolymerization of Thiol-Alkynes: Polysulfide Networks, Chem. Mater. 21 (2009) 1579-1585.
[26] J.W. Chan, C.E. Hoyle, A.B. Lowe, Sequential Phosphine-Catalyzed, Nucleophilic Thiol−Ene/Radical-Mediated Thiol−Yne Reactions and the Facile Orthogonal Synthesis of Polyfunctional Materials, J. Am. Chem. Soc. 131 (2009) 5751-5753.
[27] B.D. Fairbanks, T.F. Scott, C.J. Kloxin, K.S. Anseth, C.N. Bowman, Thiol−Yne Photopolymerizations: Novel Mechanism, Kinetics, and Step-Growth Formation of Highly Cross-Linked Networks, Macromolecules 42 (2009) 211-217.
[28] R. Cervera-Procas, C. Sánchez-Somolinos, J.L. Serrano, A. Omenat, A Polymer Network Prepared by the Thiol-yne Photocrosslinking of a Liquid Crystalline Dendrimer, Macromol. Rapid Commun. 34 (2013) 498-503.
[29] D. Martella, C. Parmeggiani, D.S. Wiersma, M. Pinol, L. Oriol, The first thiol-yne click chemistry approach for the preparation of liquid crystalline elastomers, J. Mater. Chem. C 3 (2015) 9003-9010.
[30] A.S. Quick, A. de los Santos Pereira, M. Bruns, T. Bückmann, C. Rodriguez-Emmenegger, M. Wegener, C. Barner-Kowollik, Rapid Thiol-Yne-Mediated Fabrication and Dual Postfunctionalization of Micro-Resolved 3D Mesostructures, Adv. Funct. Mater. 25 (2015) 3735-3744.
[31] A. Massi, D. Nanni, Thiol-yne coupling: revisiting old concepts as a breakthrough for up-to-date applications, Org. Biomol. Chem. 10 (2012) 3791-3807.
[32] R. Hoogenboom, Thiol-Yne Chemistry: A Powerful Tool for Creating Highly Functional Materials, Angew. Chem. Int. Ed. 49 (2010) 3415-3417.
[33] C.E. Hoyle, A.B. Lowe, C.N. Bowman, Thiol-click chemistry: a multifaceted toolbox for small molecule and polymer synthesis, Chem. Soc. Rev. 39 (2010) 1355-1387.
[34] A.B. Lowe, C.E. Hoyle, C.N. Bowman, Thiol-yne click chemistry: A powerful and versatile methodology for materials synthesis, J. Mater. Chem. 20 (2010) 4745-4750.
[35] W. Liu, C.-M. Dong, Versatile Strategy for the Synthesis of Hyperbranched Poly(ε-caprolactone)s and Polypseudorotaxanes Thereof, Macromolecules 43 (2010) 8447-8455.

[36] A. Leroy, A. Al Samad, X. Garric, S. Hunger, D. Noel, J. Coudane, B. Nottelet, Biodegradable networks for soft tissue engineering by thiol-yne photo cross-linking of multifunctional polyesters, RSC Adv. 4 (2014) 32017-32023.
[37] M. Lomba, L. Oriol, R. Alcala, C. Sanchez, M. Moros, V. Grazu, J.L. Serrano, J.M. De la Fuente, In Situ Photopolymerization of Biomaterials by Thiol-yne Click Chemistry, Macromol. Biosci. 11 (2011) 1505-1514.
[38] A. Oesterreicher, J. Wiener, M. Roth, A. Moser, R. Gmeiner, M. Edler, G. Pinter, T. Griesser, Tough and degradable photopolymers derived from alkyne monomers for 3D printing of biomedical materials, Polym. Chem. 7 (2016) 5169-5180.
[39] A. Oesterreicher, S. Ayalur-Karunakaran, A. Moser, F.H. Mostegel, M. Edler, P. Kaschnitz, G. Pinter, G. Trimmel, S. Schlögl, T. Griesser, Exploring thiol-yne based monomers as low cytotoxic building blocks for radical photopolymerization, J. Polym. Sci. Part A: Polym. Chem. 54 (2016) 3484-3494.
[40] C. Sardo, B. Nottelet, D. Triolo, G. Giammona, X. Garric, J.-P. Lavigne, G. Cavallaro, J. Coudane, When Functionalization of PLA Surfaces Meets Thiol–Yne Photochemistry: Case Study with Antibacterial Polyaspartamide Derivatives, Biomacromolecules 15 (2014) 4351-4362.
[41] S. Chevalier, C. Cuestas-Ayllon, V. Grazu, M. Luna, H. Feracci, J.M. de la Fuente, Creating Biomimetic Surfaces through Covalent and Oriented Binding of Proteins, Langmuir 26 (2010) 14707-14715.
[42] F. Nederberg, E.F. Connor, M. Moller, T. Glauser, J.L. Hedrick, New paradigms for organic catalysts: The first organocatalytic living polymerization, Angew. Chem. Int. Ed. 40 (2001) 2712-2715.